RESEARCH ARTICLE | OCTOBER 21 2024

Performance evaluation of machine learning algorithms in predicting machining responses of superalloys

Abhijit Bhowmik ; Raja Praveen K. N.; Nilesh Bhosle; Kunal Gagneja; Zunirah Mohd Talib; Jasgurpreet Singh Chohan ; Ahmed Alkhayyat; M. Janaki Ramudu; A. Johnson Santhosh

AIP Advances 14, 105027 (2024)
https://doi.org/10.1063/5.0235664

Performance evaluation of machine learning algorithms in predicting machining responses of superalloys

Cite as: AIP Advances 14, 105027 (2024); doi: 10.1063/5.0235664
Submitted: 29 August 2024 • Accepted: 24 September 2024 •
Published Online: 21 October 2024

Abhijit Bhowmik,[1,2] Raja Praveen K. N.,[3] Nilesh Bhosle,[4] Kunal Gagneja,[5] Zunirah Mohd Talib,[6] Jasgurpreet Singh Chohan,[7,8] Ahmed Alkhayyat,[9] M. Janaki Ramudu,[10] and A. Johnson Santhosh[11,a)]

AFFILIATIONS

[1]Department of Mechanical Engineering, Dream Institute of Technology, Kolkata 700104, India
[2]Centre of Research Impact and Outreach, Chitkara University, Rajpura, Punjab 140417, India
[3]Department of Computer Science and Engineering, School of Engineering and Technology, JAIN (Deemed to be University), Bangalore, Karnataka, India
[4]NIMS School of Computing Science and Artificial Intelligence, NIMS University Rajasthan, Jaipur, India
[5]Department of Computer Science and Engineering, Chandigarh Engineering College, Chandigarh Group of Colleges-Jhanjeri, Mohali, Punjab 140307, India
[6]Management and Science University, Shah Alam, Selangor, Malaysia
[7]School of Mechanical Engineering, Rayat Bahra University, Kharar, Punjab 140103, India
[8]Faculty of Engineering, Sohar University, P.O. Box 44, Sohar PCI 311, Oman
[9]College of Technical Engineering, The Islamic University, Najaf, Iraq
[10]Department of Computer Science and Engineering, Raghu Engineering College, Vishakhapatnam, Andhra Pradesh 531162, India
[11]Faculty of Mechanical Engineering, Jimma Institute of Technology, Jimma University, Jimma, Ethiopia

[a)]**Author to whom correspondence should be addressed:** johnson.antony@ju.edu.et

ABSTRACT

This study explores the application of machine learning algorithms—gene expression programming (GEP), adaptive neuro-fuzzy inference system (ANFIS), and artificial neural networks (ANN)—to predict machining responses during the milling of Inconel 690, a superalloy known for its exceptional mechanical properties and oxidation resistance. Machining Inconel 690 presents significant challenges due to its toughness and work-hardening tendencies, which can lead to rapid tool wear and poor surface finish. Traditional optimization methods often rely on empirical models and trial-and-error approaches, which are time-consuming and costly. In contrast, machine learning techniques can effectively model complex, nonlinear relationships between machining parameters and performance outcomes, such as surface roughness, cutting force, and cutting temperature. This study employs statistical metrics, including Root mean square error (RMSE), coefficient of determination (R^2), and mean absolute percentage error (MAPE), to determine the predictive performance of the models. The results show that the GEP model achieved an R^2 ranging from 0.944 572 to 0.992 999, with an RMSE between 0.015 527% and 0.694 523% and a MAPE ranging from 1.452 397% to 4.947 892%. ANFIS and ANN also demonstrated strong predictive capabilities, although GEP outperformed them. The importance of this study lies in its demonstration of advanced AI techniques as effective tools for optimizing machining processes, ultimately contributing to improved efficiency and quality in manufacturing superalloys.

I. INTRODUCTION

The rapid progress in manufacturing technologies has heightened the emphasis on enhancing the efficiency and quality of machining processes, particularly for high-performance materials such as superalloys. Superalloys, including Inconel 690, are extensively utilized in aerospace, nuclear, and chemical industries due to their exceptional mechanical properties, high oxidation resistance, and ability to retain structural integrity at elevated temperatures.[1–3] However, machining these materials poses significant challenges due to their toughness, high strength, and tendency to work-harden, leading to accelerated tool wear and suboptimal surface finishes.[4–6] As a result, optimizing machining parameters for these materials is crucial, as it can greatly influence production costs and product quality. Traditional methods for optimizing machining processes typically depend on empirical models and trial-and-error approaches, which can be both time-consuming and costly. Furthermore, these methods often fail to fully capture the intricate, nonlinear interactions between machining parameters and resulting responses such as surface roughness, cutting force, and cutting temperature. Recently, machine learning (ML) techniques have emerged as a promising alternative for predicting and optimizing machining performance. By utilizing large datasets and advanced algorithms, ML models can identify complex data patterns and make accurate predictions, thereby reducing the reliance on extensive experimentation.[7–11]

Sahoo *et al.*[12] employed three-dimensional surface plots and developed models for surface roughness using response surface methodology (RSM) and neural networks, focusing on the effects of cutting speed, feed rate, and depth of cut during dry turning of AISI 1040 steel. Their results indicated a strong correlation between the predicted and experimental roughness values for both models. Similarly, Sahin and Motorcu[13] explored surface quality during hard turning with cubic boron nitride tools, determining that feed rate was the most critical factor. Their RSM-based model proved highly accurate in predicting surface roughness. In another study, Singh and Rao[14] analyzed the influence of tool geometry and cutting parameters on surface roughness in the hard turning of AISI 52100 steel, using surface plots and RSM-based mathematical models. Marani Barzani *et al.*[15] adopted a different approach by using a fuzzy logic-based model to predict surface roughness during the turning of casting alloys, achieving a prediction accuracy of 94.6%. Chakala *et al.*[16] investigated the predictive abilities of artificial neural networks (ANN) and adaptive neuro-fuzzy inference system (ANFIS) models for wire electrical discharge machining (WEDM) of NITINOL shape memory alloys (SMA), with a focus on material removal rate (MRR) and surface roughness (SR). Kalyan *et al.*[17] used RSM and ANN to model parameters for laser assisted turning of Inconel 718, finding that the ANN model offered superior accuracy compared to RSM. Unune and Mali[18] also compared ANN and RSM models, concluding that ANN provided a more accurate match with empirical data, especially in the context of electrical discharge diamond grinding of Inconel 718 superalloy. Ranganathan *et al.*[19] assessed the machinability of hardened steel using both coated carbide and ceramic inserts, noting that ANN was more precise in predicting surface roughness and cutting force compared to other modeling techniques. Sen *et al.*[20] investigated the machining challenges of Inconel 690, characterized by low thermal conductivity and poor machinability, leading to high tool wear and machining costs. This study introduces an AI-driven meta-model for accurately predicting maximum flank wear, validated through experiments with a TiAlN-coated solid carbide insert. The findings indicate that the gene expression programming (GEP) model outperformed the ANN model, offering valuable insights into predicting tool wear in the metal-cutting industry.

Recent studies highlight the growing effectiveness of AI-based predictive models, such as ANN, RSM, and ANFIS, as powerful tools for surrogate modeling in machining processes. ANN has become particularly popular due to its ability to model complex non-linear relationships. However, the performance of these AI models largely depends on optimizing their architecture and selecting suitable learning algorithms to address challenges such as non-linearity and overfitting. Meanwhile, GEP, an evolutionary algorithm, has garnered attention for its ability to evolve symbolic expressions that accurately represent intricate relationships between input and output variables.[21–23] This makes GEP a promising option for modeling the complex dynamics of machining processes, although it remains less explored compared to ANN and RSM. This study conducts a comprehensive comparison of GEP, ANN, and ANFIS models to evaluate their effectiveness in predicting machining responses for Inconel 690, a superalloy widely used in high-performance industries. The primary goal is to assess the models' predictive accuracy, reliability, and generalizability using statistical metrics such as root mean square error (RMSE), the coefficient of determination (R^2), and mean absolute percentage error (MAPE). These metrics provide critical insights into the models' ability to generalize from training data, offering the potential for real-world application in optimizing machining processes. The research findings are expected to contribute significantly to the application of machine learning in manufacturing, particularly in machining difficult-to-machine materials like superalloys.

II. EXPERIMENTAL INVESTIGATION

The experiment was carried out on a CNC-assisted 3-axis milling machine, operating without any cutting fluid. The experimental setup was organized based on the RSM methodology, as presented in Tables I and II. Machining was conducted using an uncoated solid carbide cutter under dry conditions, with consistent parameters for cutting speed, feed rate, depth of cut, and width of cut. The 29 samples used in the experiment each measured 60 mm

TABLE I. Experimental levels of the independent variables along with their corresponding coding (dataset 1).

Factor /level	Cutting speed (m/min)	Feed (mm/tooth)	Depth of cut (mm)	Width of cut (mm)
−1	100	0.1	0.5	0.2
0	120	0.15	0.75	1
1	140	0.2	1	1.8

TABLE II. Experimental levels of the independent variables along with their corresponding coding (dataset 2).

Factor /level	Cutting speed (m/min)	Feed (mm/tooth)	Depth of cut (mm)	Width of cut (mm)
−1	80	0.05	0.25	0.1
0	100	0.1	0.5	0.9
1	120	0.15	0.75	1.7

in length and 40 mm in width. A detailed summary of the experimental cutting conditions, including the cutting tool geometry, is presented in Table III.

The samples were machined using a CNC milling machine, crafted by MTAB Engineers Pvt. Ltd. This advanced milling apparatus provided the necessary precision and control required for our experimental procedures. The evaluation of surface roughness was carried out using a sophisticated 3D profilometer, which operates at a magnification of 20×. This high level of magnification allowed for detailed surface analysis, ensuring accurate measurements. The profilometer was set with a cutoff distance of ~4.7 mm, a critical parameter for obtaining reliable data on the surface texture of the machined samples.

In addition, a crucial factor of interest was the cutting force encountered along the direction of the tool's movement. This was precisely measured using a dynamometer, an instrument designed to capture the force dynamics during the machining process. Accurate force measurement is essential for understanding the interactions between the cutting tool and the material, which, in turn, influences the overall machinability and performance outcomes. Finally, for the measurement of cutting temperature, a specially developed infrared (IR) camera was utilized. This cutting-edge device allowed for non-contact, real-time temperature measurements, providing crucial insights into the thermal effects experienced during the machining process. The IR camera, with its high spatial and temporal resolution, ensured accurate and continuous monitoring of the cutting zone. Monitoring the cutting temperature is vital, as excessive heat can adversely affect the material properties and tool life. Figure 1 shows the schematic representation of the current study.

TABLE III. Specifications of the experimental setup and tool design.

Machine tool	Tool material	Cutter length	Cutter diameter	Flutes	Length of a flute	Coolant
CNC milling machine	Uncoated solid carbide mill cutter	7.5 cm	0.8 cm	4	2.5 cm	Dry machining condition

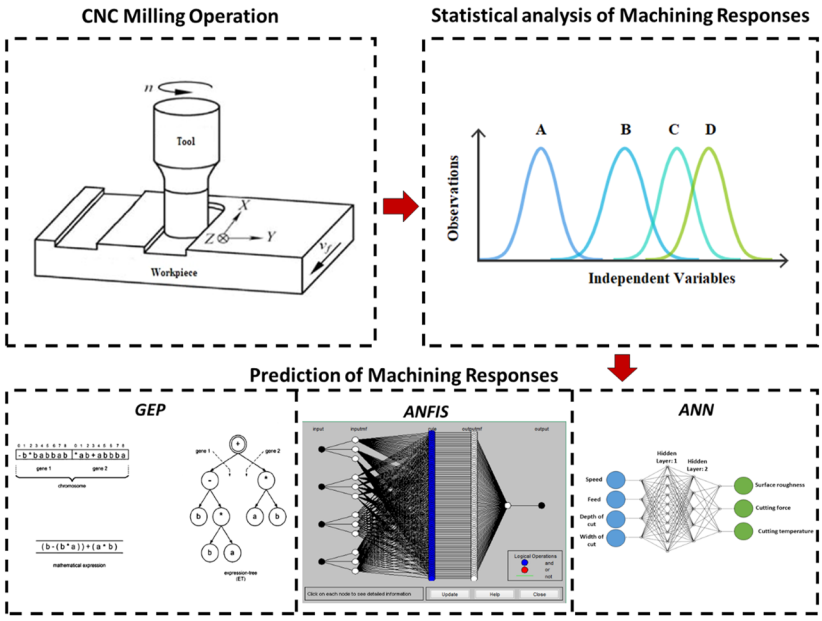

FIG. 1. Schematic diagram of the contemporary study.

III. PREDICTIVE MODELING TECHNIQUES

A. GEP

GEP is an evolutionary algorithm introduced by Candida Ferreira in 2001.[24] It integrates concepts from both genetic algorithms and genetic programming. GEP aims to evolve computer programs or models that can perform specific tasks or solve problems by mimicking the natural process of evolution.[25–29] At its core, GEP operates based on encoding solutions into linear chromosomes, which are then evaluated and evolved through selection, crossover, and mutation operations.[30–32] These chromosomes are represented in a linear form, but they can be decoded into complex expression trees, allowing GEP to generate and optimize various types of models, such as mathematical functions or symbolic expressions.[33,34]

The key features of GEP include its ability to handle both numerical and symbolic data and its flexibility in evolving diverse types of functions and models. The linear chromosomes in GEP are composed of genes, each containing a set of instructions or functions. These genes are assembled into a linear genome, which is then translated into expression trees or mathematical expressions. This approach allows GEP to efficiently explore and exploit the solution space by evolving solutions through a process of recombination and mutation.[35,36] GEP has several advantages, such as its ability to represent complex solutions in a concise manner, its robustness in handling noisy or incomplete data, and its versatility in generating both analytical and empirical models. In addition, GEP's capacity to evolve models with minimal prior knowledge makes it a powerful tool in various problem-solving scenarios.[37–39] Overall, GEP is a potent evolutionary algorithm that leverages genetic principles to evolve effective models and solutions, providing a valuable approach for tackling complex and diverse problems in computational fields. Figure 2 shows the steps involved in GEP.

B. ANFIS

ANFIS is a sophisticated intelligent system that integrates neural networks with fuzzy logic to enhance the modeling of intricate and nonlinear systems. It combines the adaptive learning features of neural networks with the interpretative and reasoning strengths of fuzzy logic, enabling it to effectively model ambiguous or imprecise information through the use of fuzzy sets and rules.[40,41] Fuzzy inference systems utilize linguistic variables and fuzzy rules to convert inputs into outputs, mimicking human reasoning. The neural network component of ANFIS plays a crucial role in optimizing the fuzzy system's parameters, using a learning algorithm to adjust membership functions and the rule base based on input–output data.[42,43] ANFIS is generally organized into five layers.

(a) Input Layer: receives input data and represents it in fuzzy terms through membership functions.
(b) Rule Layer: applies fuzzy rules to inputs to determine firing strengths.
(c) Normalization Layer: adjusts the firing strengths of the rules so that their total equals one.
(d) Defuzzification Layer: combines the rule outputs to produce a unified output.
(e) Output Layer: delivers the final output using defuzzification methods.

Through its training mechanism, ANFIS modifies the parameters of membership functions and rules to reduce the error between predicted and actual outputs. This flexibility allows ANFIS to effectively manage complex system modeling tasks. By merging the qualitative insights of fuzzy logic with the quantitative learning capabilities of neural networks, ANFIS achieves a balance between interpretability and precision in its modeling approach. A flow chart of the ANFIS model is shown in Fig. 3.

C. ANN

ANNs are computational models inspired by the neural structures of the human brain. They consist of layers of interconnected nodes, known as "neurons," which perform fundamental calculations. Typically, an ANN includes an input layer, one or more

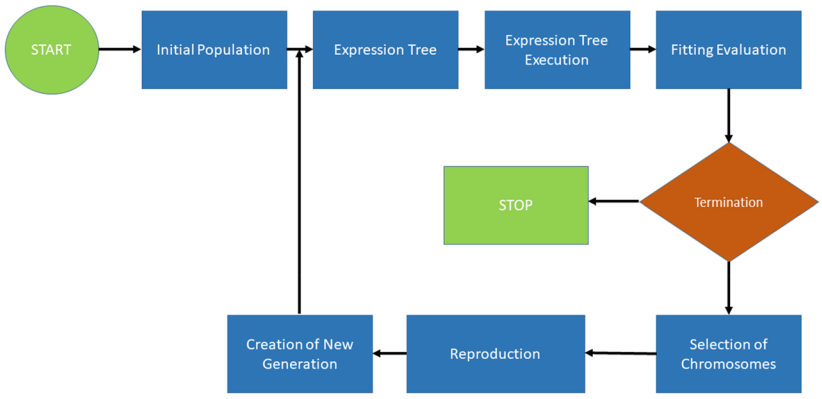

FIG. 2. Flow chart of the GEP algorithm.

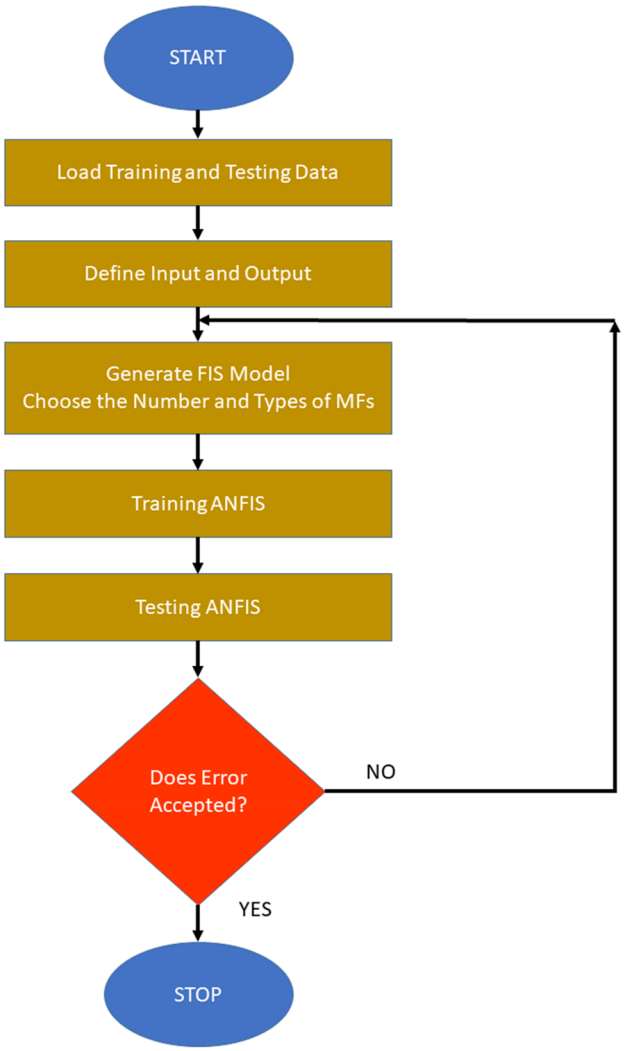

FIG. 3. Diagram illustrating the ANFIS process.

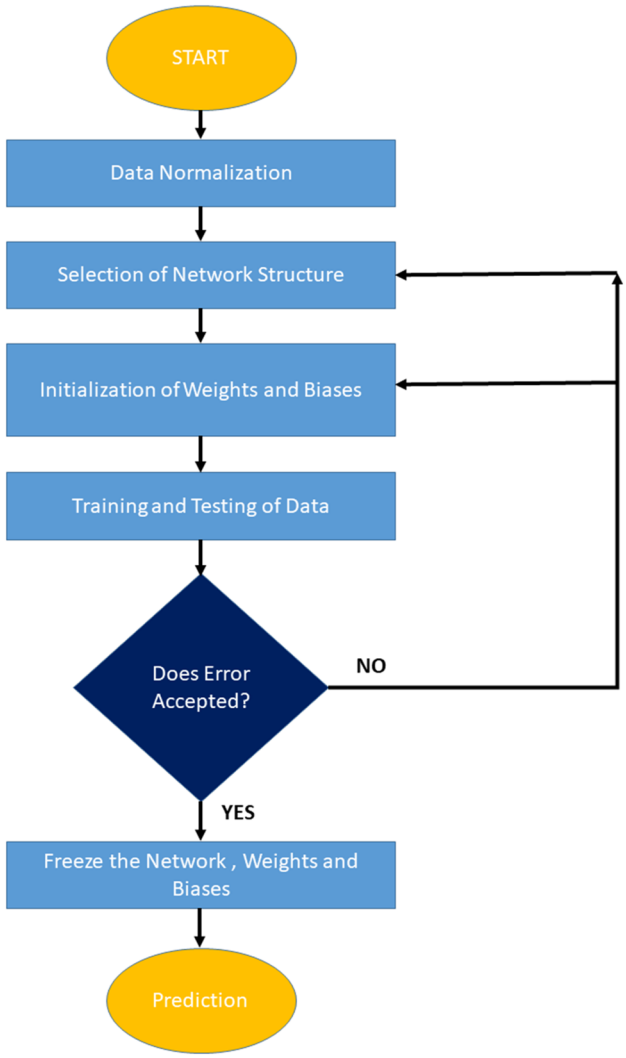

FIG. 4. Flow chart of the utilized ANN for predicting machining responses.

hidden layers, and an output layer.[44–46] The neurons in the input layer receive and weigh incoming signals, which are then passed to neurons in the hidden layers. These hidden neurons apply an activation function to the weighted sum of their inputs, generating an output that is forwarded to subsequent layers. This iterative process continues until the final result is produced by the output layer. During the training phase, the network's connection weights are adjusted to minimize the difference between the predicted and actual outcomes.[47,48]

Training an ANN typically involves the backpropagation method. This approach calculates the prediction error and propagates it backward through the network to update the weights using optimization techniques, such as gradient descent. This process is repeated until the network's performance stabilizes and achieves a satisfactory accuracy level. ANNs are highly adaptable and capable of modeling complex, non-linear relationships between inputs and outputs. They can handle various types of data and adjust to new patterns by modifying their weights and biases. This adaptability makes ANNs crucial in machine learning and artificial intelligence for applications such as pattern recognition, classification, regression, and time-series forecasting.[49] Figure 4 shows the process of ANN modeling.

D. Performance assessment of predictive models

In examining a substantial body of research concerning the application of AI models for mapping machining performance parameters in CNC milling, it has been observed that these AI models are commonly evaluated using statistical metrics, such as the R^2, RMSE, and MAPE [Eqs. (1)–(3)]. RMSE and MAPE, in particular, quantify the deviation between experimental and predicted values. These deviations, known as residuals, are integral to assessing the accuracy

of predictive models, making RMSE and MAPE essential tools for comparing the predictive errors of different AI models,

$$R^2 = 1 - \left(\frac{\sum_{i=1}^{n} (E_i - P_i)^2}{\sum_{i=1}^{n} (P_i)^2} \right), \quad (1)$$

$$\text{RMSE} = \sqrt{\frac{1}{n} \sum_{i=1}^{n} (E_i - P_i)^2}, \quad (2)$$

$$\text{MAPE} = \frac{1}{n} \sum_{i=1}^{n} \left(\frac{E_i - P_i}{E_i} \right) * 100. \quad (3)$$

In this context, "n" represents the total number of patterns within the dataset, "E" denotes the output obtained from experiments, and 'P' refers to the value predicted by the model.

IV. RESULTS AND DISCUSSION

A. Statistical analysis of experimental data

This study utilized ANOVA[50] to evaluate the influences of various input parameters on machining performance. ANOVA, chosen for its robustness, was conducted with a 95% confidence level to ensure result reliability. The analysis employed Minitab 19, a sophisticated statistical software. Within the ANOVA framework, Fisher's F-test quantified the variance attributed to each machining parameter and assessed their impact on performance metrics. The F-value from this test indicates the strength of the relationship between input parameters and performance outcomes, with a larger F-value denoting a more significant effect. The p-value associated with the F-test determined the statistical importance of the results. A p-value less than 0.05 directed statistically significant effects, suggesting that the observed results were unlikely due to chance. This approach ensured the identification and confirmation of key parameters' relevance with high statistical confidence.

The ANOVA analysis for both dataset 1 and dataset 2 reveals that machining parameters significantly affect surface roughness, cutting force, and cutting temperature. In dataset 1 (Table IV), surface roughness is notably influenced by feed and depth-of-cut, with p-values of 0.002 and 0.003, respectively, while speed and width-of-cut do not have a significant impact. For cutting force, feed and depth-of-cut are the primary factors, with p-values of 0.023 and 0.001, respectively, whereas speed and width-of-cut do not contribute significantly. Cutting temperature is affected by all parameters except width-of-cut, with speed, feed, and depth-of-cut

TABLE IV. ANOVA for response parameters (dataset 1).

Source	DOF	Adj. SS	Adj. MS	F- value	P-value
Surface roughness					
Speed	1	0.000 075	0.000 075	4.330	0.056
Feed	1	0.007 351	0.007 351	425.86	0.002
Depth-of-cut	1	0.623 550	0.062 355	361.29	0.003
Width-of-cut	1	0.548 610	0.001 473	1.456	0.895
Cutting force					
Speed	1	234	233.5	2.76	0.119
Feed	1	470.34	47 034.4	556.21	0.023
Depth-of-cut	1	550.16	55 015.7	650.59	0.001
Width-of-cut	1	68.463	68 463.4	1.62	0.756
Cutting temperature					
Speed	1	28.830	28.8300	11.45	0.004
Feed	1	50.923	50.9232	20.22	0.001
Depth-of-cut	1	66.270	66.2700	26.32	0.001
Width-of-cut	1	14.520	14.5200	5.77	0.889

TABLE V. ANOVA for response parameters (dataset 2).

Source	DOF	Adj. SS	Adj. MS	F- value	P-value
Surface roughness					
Speed	1	0.000 068	0.007 750	8.220	0.049
Feed	1	0.008 341	0.007 426	329.86	0.001
Depth-of-cut	1	0.524 557	0.012 587	301.29	0.001
Width-of-cut	1	0.448 519	0.075 690	0.896	0.792
Cutting force					
Speed	1	247	337.50	3.221	0.108
Feed	1	430.37	7704.4	455.81	0.011
Depth-of-cut	1	570.89	45 005.1	790.51	0.001
Width-of-cut	1	62.773	6478.4	1.4087	0.874
Cutting temperature					
Speed	1	30.756	17.756	19.75	0.003
Feed	1	70.759	80.4530	21.75	0.002
Depth-of-cut	1	86.753	66.4259	39.307	0.001
Width-of-cut	1	14.75	17.2560	4.728	0.228

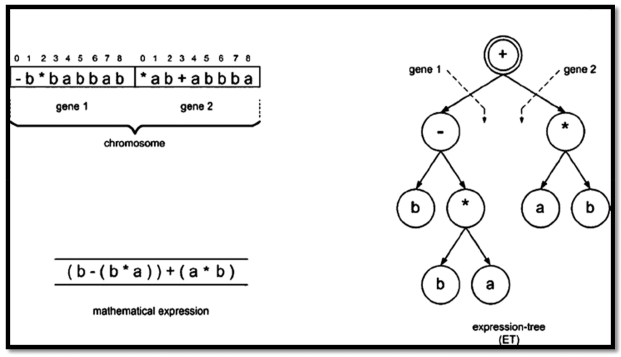

FIG. 5. Example of a GEP expression tree.

TABLE VI. Parameters for simulating the GEP model.

Parameter	Gene recombination rate	Mutation rate	Number of genes	One-point recombination rate	Number of chromosomes	Inverse rate	Linking function	Two-point recombination rate	Head size
Value	0.1	0.044	4, 5, 6	0.3	60, 70, 80	0.1	Addition	0.3	15, 20

having p-values of 0.004, 0.001, and 0.001, respectively. In dataset 2 (Table V), similar patterns emerge. Surface roughness is significantly influenced by speed, feed, and depth-of-cut, with p-values of 0.049, 0.001, and 0.001, respectively, while width-of-cut remains insignificant. Cutting force is also significantly affected by feed and depth-of-cut, with p-values of 0.011 and 0.001, with speed and width-of-cut not showing significant effects. Cutting temperature is notably influenced by speed, feed, and depth-of-cut, with p-values of 0.003, 0.002, and 0.001, respectively, while width-of-cut does not show significant impact. Across both datasets, feed and depth-of-cut consistently demonstrate a significant effect on all response parameters.

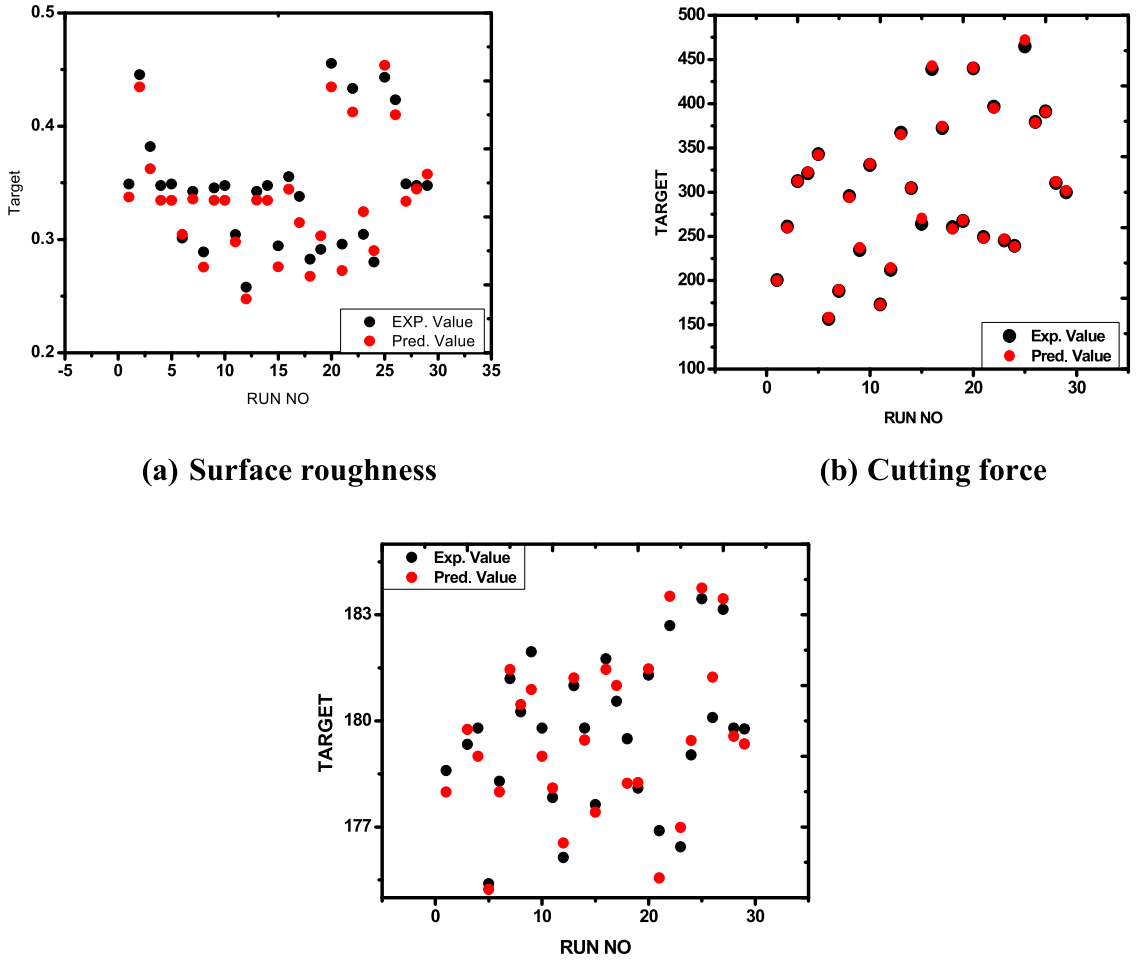

(a) Surface roughness

(b) Cutting force

(c) Cutting temperature

FIG. 6. Comparison of GEP predicted data with the measured data (dataset 1).

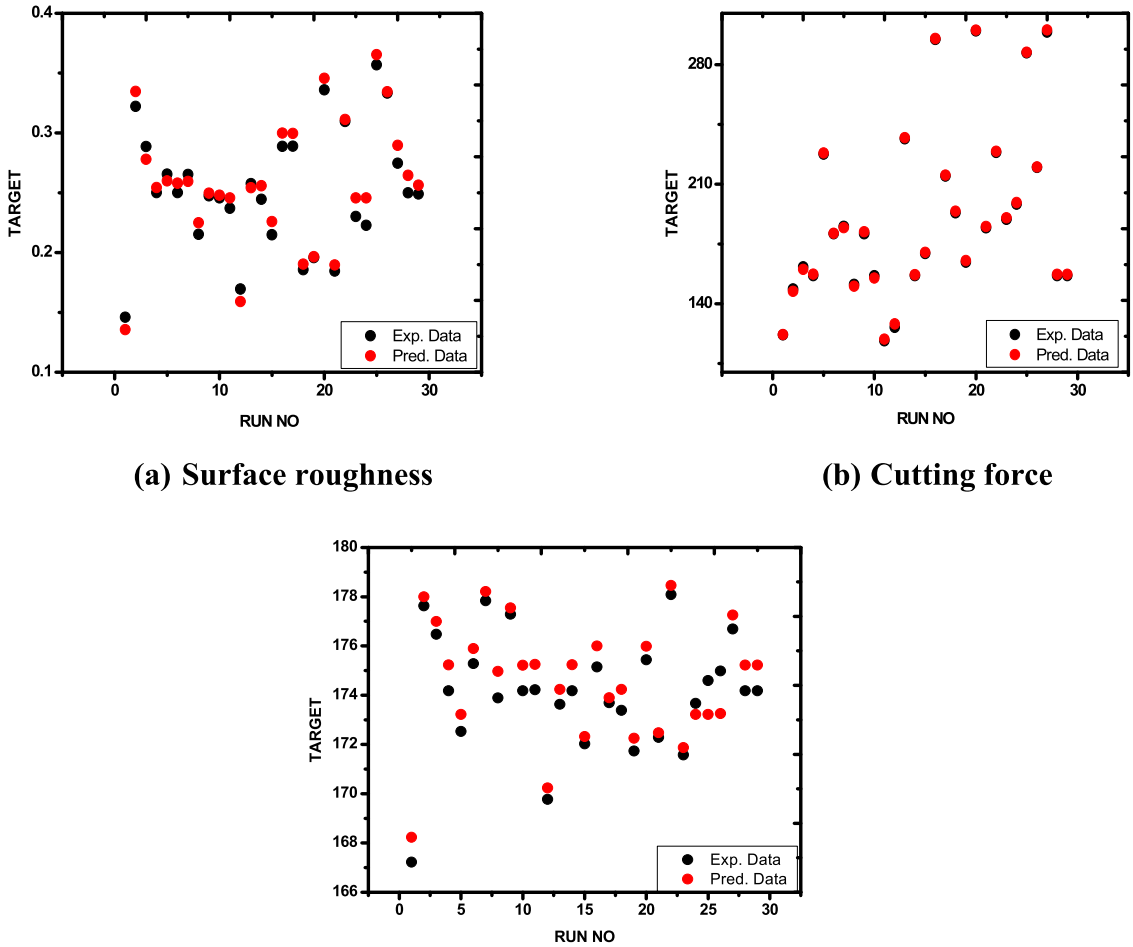

FIG. 7. Comparison of GEP predicted data with the measured data (dataset 2).

B. Results of GEP models

GEP consists of five essential elements: fitness function, stopping criteria, terminal set, control parameters, and function set, all of which are necessary for successful problem-solving. In this process, characters are usually represented as linear strings of a fixed length, referred to as genomes. These genomes are then converted into non-linear forms known as expression trees, which can vary in size and shape, as shown in Fig. 5.

In this research, the GEP model was developed using fundamental arithmetic operations alongside a variety of mathematical functions. Increasing the population size led to extended iteration periods, and the program continued running until improvements in model performance became minimal. The parameters for the GEP model simulation are presented in Table VI. For GEP to function effectively, the problem must be clearly defined. The algorithm then autonomously seeks a solution through a problem-independent approach. GEP includes a parse tree generator that converts the

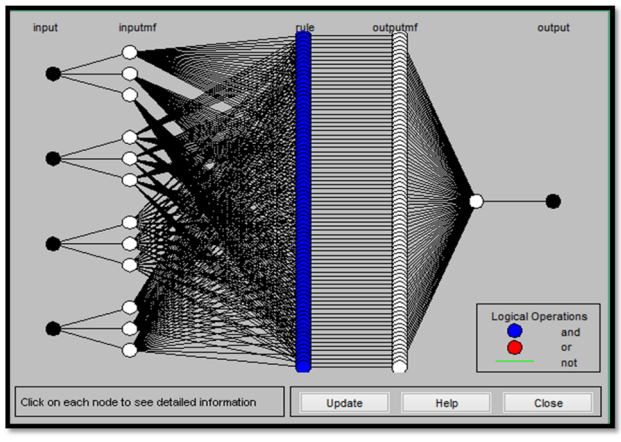

FIG. 8. Architecture of ANFIS.

native Karva code of logic circuits into graphical representations or expression trees, facilitating a more thorough understanding of their Boolean structure. Figures 6 and 7 compare GEP-predicted data with two experimental datasets, demonstrating the efficacy of the GEP model.

C. Results of ANFIS models

As previously discussed, the ANFIS structural design comprises five distinct layers (Fig. 8), each executing a specific function to facilitate signal propagation. This network structure includes numerous nodes connected through direct links. In this study, the ANFIS model was constructed within the MATLAB environment. A dataset consisting of 29 data pairs was utilized, with 15 pairs allocated for training and the remaining for validation purposes. Data normalization was performed within a range of 0 to 1. For each input variable, three different membership functions—trapezoidal, triangular, and bell-shaped—were assessed, leading to a total of 34 rules for separate ANFIS models. The model's output was derived based on these parameters, and output errors were used to refine the primary parameters through a standard backpropagation algorithm. Of the membership functions tested, the trapezoidal function exhibited the highest predictive accuracy. The ANFIS model demonstrated strong correlation metrics when predicting the CNC milling machine's output parameters, with the predicted machining parameters showing commendable precision. A detailed examination of Figs. 9 and 10 reveals a consistent and remarkable agreement between the network-predicted values and the

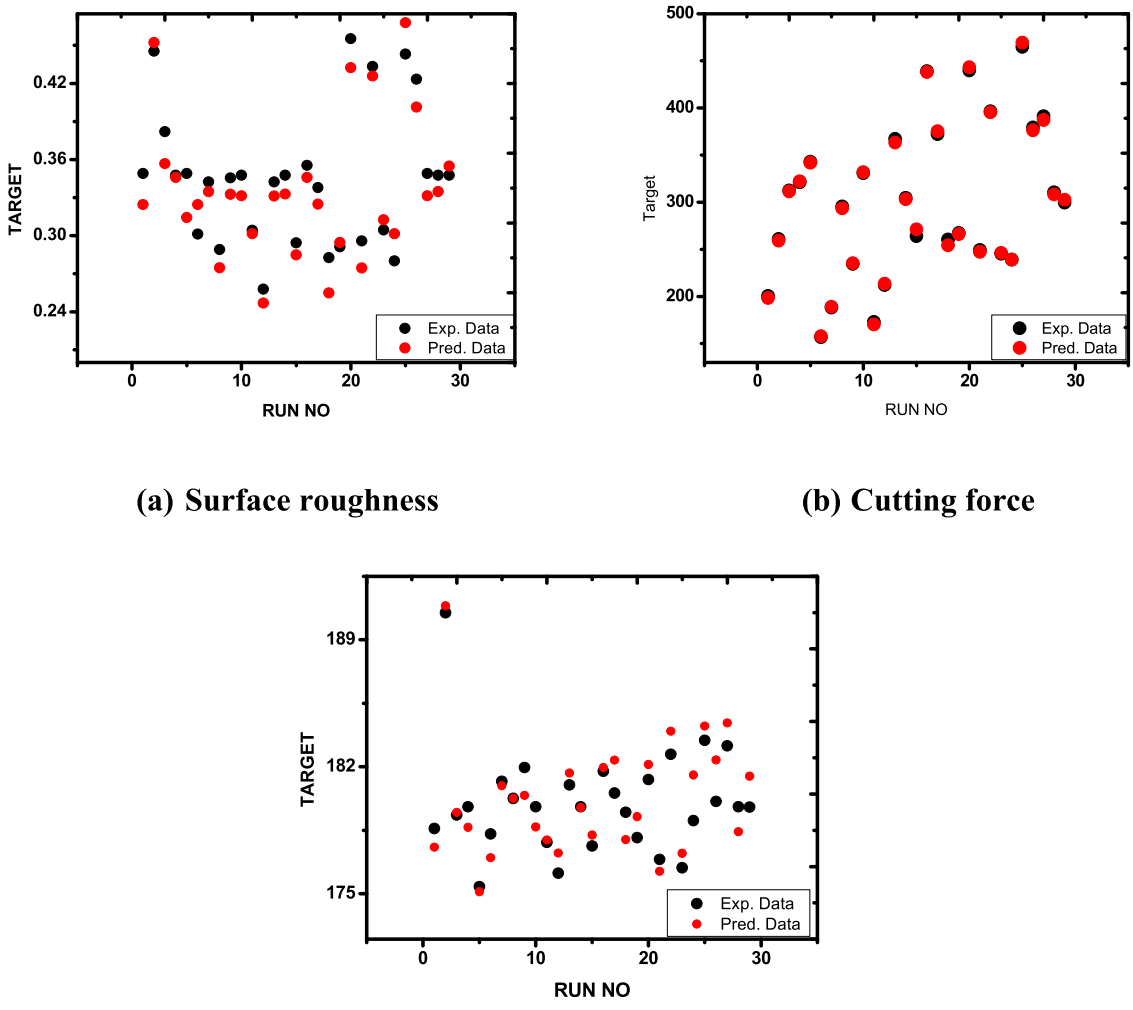

FIG. 9. Comparison of ANFIS predicted data with the measured data (dataset 1).

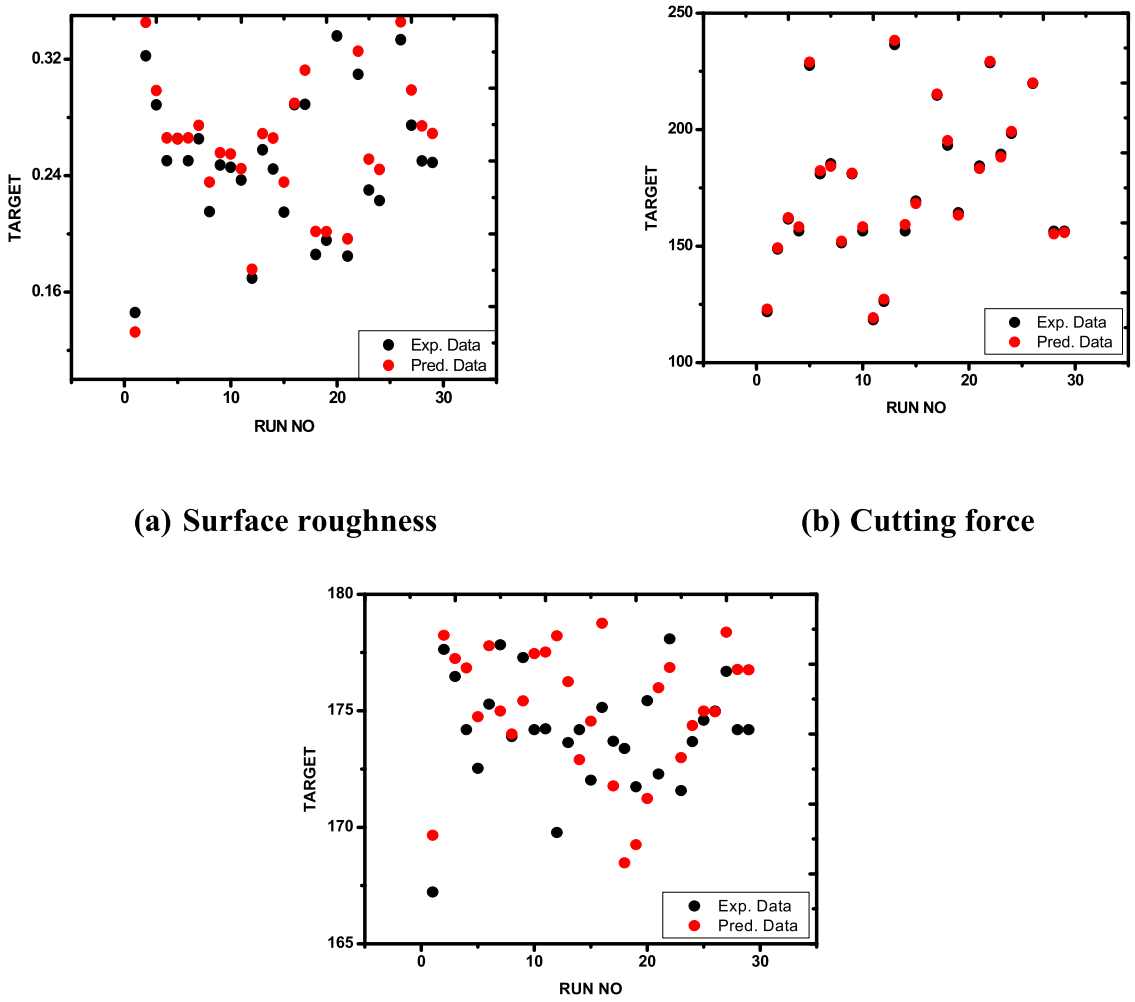

(a) Surface roughness

(b) Cutting force

(c) Cutting temperature

FIG. 10. Comparison of ANFIS predicted data with the measured data (dataset 2).

actual experimental observations throughout the entire series of operations.

D. Results of ANN models

ANN modeling also incorporated 29 experimental data points. The input parameters for the network included machining parameters. To achieve a precise and dependable model, machining responses were estimated using a perceptron neural network. Data normalization was applied to scale the data between 0.1 and 0.9. This normalization is essential for the optimal performance of soft computing techniques, addressing the considerable variations in the mathematical values of the input data.

Different neural network architectures vary based on their structure, functionality, and training methods. In this research, a feedforward neural network was trained using the backpropagation learning technique. The network's effectiveness has been calculated by measuring the discrepancy between the actual and predicted results. Comprehensive details on the network's topology and training parameters are shown in Fig. 11. The network was configured with a hyperbolic tangent activation function and comprised two hidden layers, with 10 and 5 nodes, respectively, to model the machining process outcomes. The selection of nodes and layers was optimized through iterative testing. Figures 12 and 13 show a comparison of the ANN's predictions with experimental data, indicating a close match between the predicted and actual results.

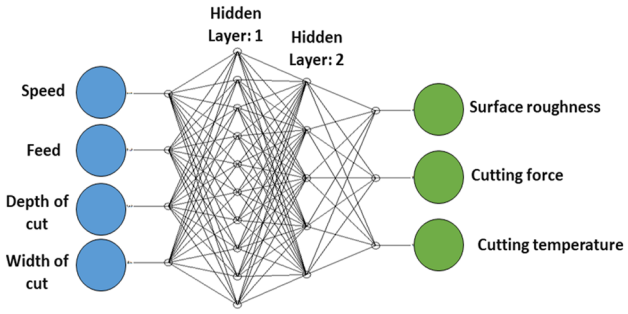

FIG. 11. Architecture of the ANN model.

E. Comparative assessment of predictive models

Three machine learning techniques were employed to forecast cutting force, surface roughness, and cutting temperature for Inconel 690. To assess and contrast the effectiveness of these models, performance metrics, such as MAPE, R^2, and RMSE, were utilized. Tables VII and VIII present the comparative results of the predictive models for Inconel 690. The GEP model, when predicting surface roughness against experimental data, achieved an R^2 between 0.944 572 and 0.992 999, an RMSE between 0.015 527% and 0.694 523%, and a MAPE between 1.452 397% and 4.947 892%. In contrast, the ANFIS model yielded an R^2 from 0.941 697 to 0.988 996, with an RMSE ranging from 0.039 470% to 0.867 622% and a MAPE from 3.541 297% to 7.456 275%. The ANN model produced an R^2 between

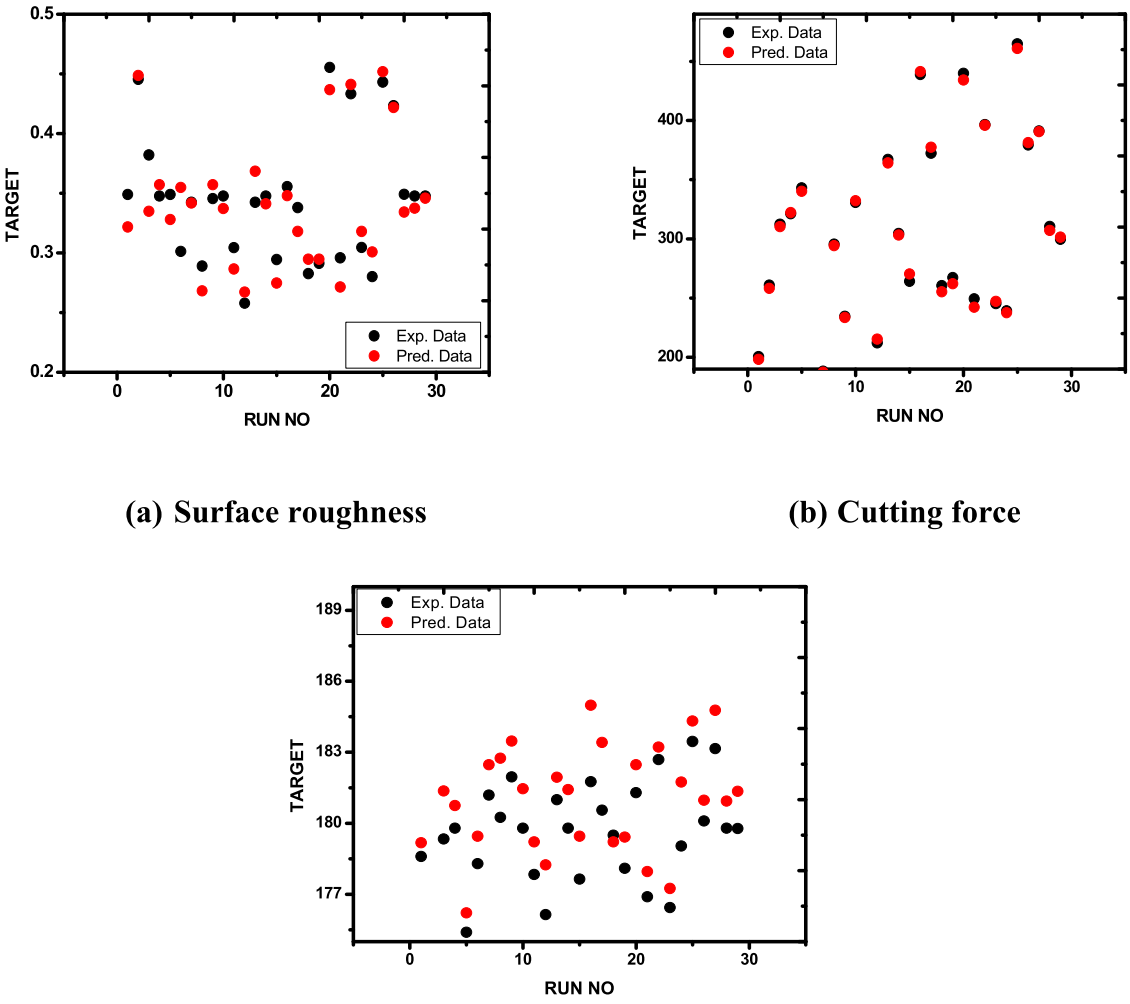

FIG. 12. Comparison of ANN-predicted data with the measured data (dataset 1).

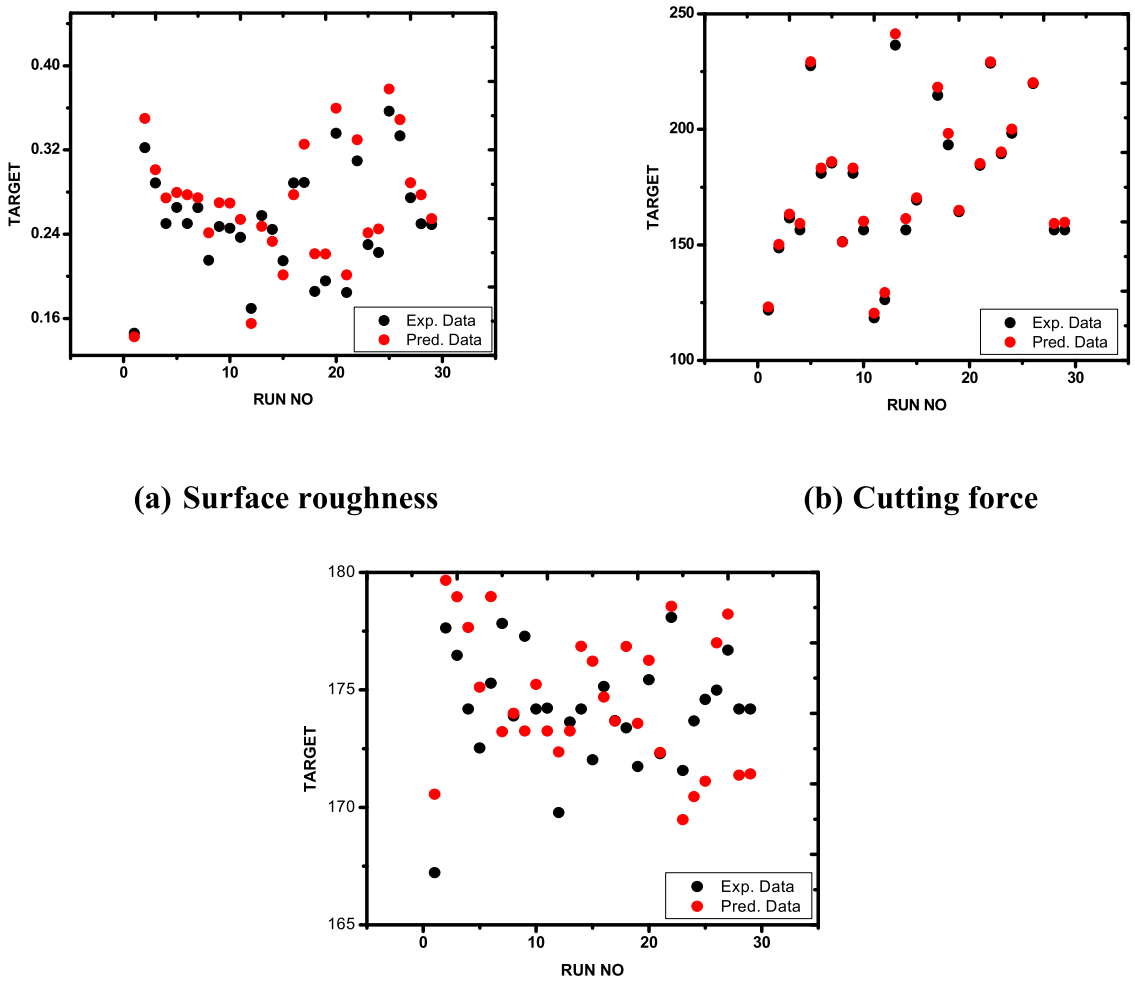

(a) Surface roughness

(b) Cutting force

(c) Cutting temperature

FIG. 13. Comparison of ANN-predicted data with the measured data (dataset 2).

TABLE VII. Comparison between predictive models (dataset 1).

Parameter	Cutting force (N)			Surface roughness (μm)			Cutting temperature (°C)		
Model	GEP	ANFIS	ANN	GEP	ANFIS	ANN	GEP	ANFIS	ANN
RMSE (%)	0.017 29	0.044 8	0.049 96	0.445 78	0.455 36	0.564 24	0.694 52	0.745 63	0.758 64
R^2	0.990 79	0.989	0.955 63	0.980 28	0.977 75	0.965 78	0.954 53	0.946 54	0.944 86
MAPE (%)	1.814 44	4.684 09	4.875 46	1.979 75	3.879 65	4.587 46	4.235 79	7.456 28	6.998 55

TABLE VIII. Comparison between predictive models (dataset 2).

Parameter	Cutting force (N)			Surface roughness (μm)			Cutting temperature (°C)		
Model	GEP	ANFIS	ANN	GEP	ANFIS	ANN	GEP	ANFIS	ANN
RMSE (%)	0.015 527	0.039 47	0.052 25	0.372 88	0.552 34	0.549 28	0.597 79	0.867 62	0.868 44
R^2	0.992 999	0.978 8	0.954 74	0.987 25	0.967 75	0.957 74	0.944 57	0.941 7	0.931 45
MAPE (%)	1.774 587	4.777 57	5.245 88	1.452 4	3.541 3	4.745 61	4.947 89	6.421 48	7.745 2

0.931 447 and 0.965 784, with an RMSE between 0.049 956% and 0.868 442% and a MAPE between 4.587 456% and 7.745 203%. These findings reflect a close alignment between the actual and predicted values across all models. Nevertheless, the GEP model outperforms the others, as indicated by its superior R^2, and lower RMSE and MAPE values.

V. CONCLUSIONS

The conclusions of this study affirm the effectiveness and precision of machine learning models—namely, GEP, ANFIS, and ANN—in predicting machining responses during the milling of Inconel 690. Through rigorous statistical evaluation, including metrics such as RMSE, the R^2, and MAPE, the study has demonstrated that all three models can accurately forecast critical machining performance parameters, such as surface roughness, cutting force, and cutting temperature. The GEP model, in particular, showed superior predictive capability, closely followed by ANFIS and ANN, each offering unique strengths in handling nonlinear data and complex relationships. These findings underscore the reliability of these models in optimizing machining processes, paving the way for more efficient manufacturing practices. The significance of this study lies in its application of advanced AI techniques to a challenging industrial process, showcasing their potential to enhance predictive accuracy and operational efficiency in machining superalloys. Future studies may investigate the potential for combining these models with real-time monitoring systems, enabling dynamic adjustments during machining to further improve outcomes. In addition, expanding the scope of this study to include different superalloys and cutting conditions could offer deeper insights into the generalizability of these models across various manufacturing environments.

AUTHOR DECLARATIONS

Conflict of Interest

The author has no conflicts to disclose.

Author Contributions

All authors listed have significantly contributed to the development and the writing of this article.

Abhijit Bhowmik: Conceptualization (equal); Data curation (equal); Formal analysis (equal); Investigation (equal); Methodology (equal); Resources (equal); Software (equal); Validation (equal); Writing – original draft (equal); Writing – review & editing (equal). **Raja Praveen K. N.**: Conceptualization (equal); Investigation (equal); Resources (equal); Software (equal); Validation (equal); Writing – review & editing (equal). **Nilesh Bhosle**: Data curation (equal); Investigation (equal); Software (equal); Validation (equal); Writing – review & editing (equal). **Kunal Gagneja**: Formal analysis (equal); Methodology (equal); Software (equal); Validation (equal); Visualization (equal); Writing – review & editing (equal). **Zunirah Mohd Talib**: Formal analysis (equal); Resources (equal); Software (equal); Visualization (equal); Writing – original draft (equal); Writing – review & editing (equal). **Jasgurpreet Singh Chohan**: Conceptualization (equal); Data curation (equal); Investigation (equal); Resources (equal); Supervision (equal); Validation (equal); Writing – review & editing (equal). **Ahmed Alkhayyat**: Data curation (equal); Funding acquisition (equal); Methodology (equal); Resources (equal); Validation (equal); Writing – review & editing (equal). **M. Janaki Ramudu**: Conceptualization (equal); Methodology (equal); Software (equal); Validation (equal); Writing – review & editing (equal). **A. Johnson Santhosh**: Conceptualization (equal); Formal analysis (equal); Methodology (equal); Software (equal); Validation (equal); Writing – review & editing (equal).

DATA AVAILABILITY

The data that support the findings of this study are available within the article.

REFERENCES

[1]B. Sen and A. Bhowmik, "Application of minimum quantity GnP nanofluid and cryogenic LN_2 in the machining of Hastelloy C276," Tribol. Int. **194**, 109509 (2024).
[2]Z. Chen, C. Huang, B. Li, G. Jiang, Z. Tang, J. Niu, and H. Liu, "Experimental study on surface integrity of Inconel 690 milled by coated carbide inserts," Int. J. Adv. Des. Manuf. Technol. **121**(5–6), 3025–3042 (2022).
[3]J. Liu, J. Xu, K. Paik, P. He, and S. Zhang, "In-situ isothermal aging TEM analysis of a micro Cu/ENIG/Sn solder joint for flexible interconnects," J. Mater. Sci. Technol. **169**, 42–52 (2024).
[4]B. Sen, M. Mia, U. K. Mandal, and S. P. Mondal, "Synergistic effect of silica and pure palm oil on the machining performances of Inconel 690: A study for promoting minimum quantity nano doped-green lubricants," J. Cleaner Prod. **258**, 120755 (2020).
[5]M. A. Makhesana, K. M. Patel, and N. Khanna, "Analysis of vegetable oil-based nano-lubricant technique for improving machinability of Inconel 690," J. Manuf. Processes **77**, 708–721 (2022).
[6]J. Song, Y. Chen, X. Hao, M. Wang, Y. Ma, and J. Xie, "Microstructure and mechanical properties of novel Ni–Cr–Co-based superalloy GTAW joints," J. Mater. Res. Technol. **29**, 2758–2767 (2024).
[7]F. Aggogeri, N. Pellegrini, and F. L. Tagliani, "Recent advances on machine learning applications in machining processes," Appl. Sci. **11**(18), 8764 (2021).
[8]M. P. Motta, C. Pelaingre, A. Delamézière, L. B. Ayed, and C. Barlier, "Machine learning models for surface roughness monitoring in machining operations," Procedia CIRP **108**, 710–715 (2022).
[9]Z. Wang, Y. Yuan, S. Zhang, Y. Lin, and J. Tan, "A multi-state fusion informer integrating transfer learning for metal tube bending early wrinkling prediction," Appl. Soft Comput. **151**, 110991 (2024).
[10]B. Sen, U. K. Mandal, and S. P. Mondal, "Advancement of an intelligent system based on ANFIS for predicting machining performance parameters of Inconel 690—A perspective of metaheuristic approach," Measurement **109**, 9–17 (2017).
[11]Z. Yang, C. Chen, D. Li, Y. Wu, Z. Geng, V. Konakov, and K. Zhou, "An additively manufactured heat-resistant Al–Ce–Sc–Zr alloy: Microstructure, mechanical properties and thermal stability," Mater. Sci. Eng.: A **872**, 144965 (2023).
[12]A. Sahoo, A. Rout, and D. Das, "Response surface and artificial neural network prediction model and optimization for surface roughness in machining," Int. J. Ind. Eng. Comput. **6**(2), 229–240 (2015).
[13]Y. Sahin and A. R. Motorcu, "Surface roughness model in machining hardened steel with cubic boron nitride cutting tool," Int. J. Refract. Met. Hard Mater. **26**(2), 84–90 (2008).
[14]D. Singh and P. V. Rao, "A surface roughness prediction model for hard turning process," Int. J. Adv. Des. Manuf. Technol. **32**, 1115–1124 (2007).
[15]M. Marani Barzani, E. Zalnezhad, A. A. Sarhan, S. Farahany, and S. Ramesh, "Fuzzy logic based model for predicting surface roughness of machined

Al–Si–Cu–Fe die casting alloy using different additives-turning," Measurement **61**, 150–161 (2015).
[16]N. Chakala, P. S. Chandrabose, and C. S. P. Rao, "Optimisation of WEDM parameters on Nitinol alloy using RSM and desirability approach," Aust. J. Mech. Eng. **19**(5), 582–594 (2021).
[17]P. Kalyan, P. kumar, and K. Venkatesan, "Predictive modeling of laser assisted hybrid machining parameters of Inconel 718 alloy using statistical and artificial neural network," Mater. Today: Proc. **5**(5), 11248–11259 (2018).
[18]D. R. Unune and H. S. Mali, "Artificial neural network–based and response surface methodology–based predictive models for material removal rate and surface roughness during electro-discharge diamond grinding of Inconel 718," Proc. Inst. Mech. Eng., Part B **230**(11), 2082–2091 (2016).
[19]S. Ranganathan, T. Senthilvelan, and G. Sriram, "Evaluation of machining parameters of hot turning of stainless steel (Type 316) by applying ANN and RSM," Mater. Manuf. Processes **25**(10), 1131–1141 (2010).
[20]B. Sen, M. Mia, U. K. Mandal, and S. P. Mondal, "GEP- and ANN-based tool wear monitoring: A virtually sensing predictive platform for MQL-assisted milling of Inconel 690," Int. J. Adv. Des. Manuf. Technol. **105**, 395–410 (2019).
[21]B. Sen, S. Debnath, and A. Bhowmik, "Sustainable machining of superalloy in minimum quantity lubrication environment: Leveraging GEP-PSO hybrid optimization algorithm," Int. J. Adv. Des. Manuf. Technol. **130**(9–10), 4575–4601 (2024).
[22]C. Yuhua, M. Yuqing, L. Weiwei, and H. Peng, "Investigation of welding crack in micro laser welded NiTiNb shape memory alloy and Ti6Al4V alloy dissimilar metals joints," Opt Laser. Technol. **91**, 197–202 (2017).
[23]Y. Chen, S. Sun, T. Zhang, X. Zhou, and S. Li, "Effects of post-weld heat treatment on the microstructure and mechanical properties of laser-welded NiTi/304SS joint with Ni filler," Mater. Sci. Eng.: A **771**, 138545 (2020).
[24]C. Ferreira, "Gene expression programming: A new adaptive algorithm for solving problems," arXiv:cs/0102027 (2001).
[25]M. A. Ali Khan, A. Zafar, A. Akbar, M. F. Javed, and A. Mosavi, "Application of gene expression programming (GEP) for the prediction of compressive strength of geopolymer concrete," Materials **14**(5), 1106 (2021).
[26]A. Nazari and F. Pacheco Torgal, "Modeling the compressive strength of geopolymeric binders by gene expression programming-GEP," Expert Syst. Appl. **40**(14), 5427–5438 (2013).
[27]J. Zhong, L. Feng, and Y. S. Ong, "Gene expression programming: A survey [review article]," IEEE Comput. Intell. Mag. **12**(3), 54–72 (2017).
[28]H. T. He, J. X. Fang, J. X. Wang, T. Sun, Z. Yang, B. Ma, H. Chen, and M. Wen, "Carbide-reinforced $Re_{0.1}Hf_{0.25}NbTaW_{0.4}$ refractory high-entropy alloy with excellent room and elevated temperature mechanical properties," Int. J. Refract. Met. Hard Mater. **116**, 106349 (2023).
[29]Y. T. Li, X. Jiang, X. T. Wang, and Y. X. Leng, "Integration of hardness and toughness in $(CuNiTiNbCr)N_x$ high entropy films through nitrogen-induced nanocomposite structure," Scr. Mater. **238**, 115763 (2024).
[30]D. P. N. Kontoni, K. C. Onyelowe, A. M. Ebid, H. Jahangir, D. Rezazadeh Eidgahee, A. Soleymani, and C. Ikpa, "Gene expression programming (GEP) modelling of sustainable building materials including mineral admixtures for novel solutions," Mining **2**(4), 629–653 (2022).
[31]A. Ahmad, K. Chaiyasarn, F. Farooq, W. Ahmad, S. Suparp, and F. Aslam, "Compressive strength prediction via gene expression programming (GEP) and artificial neural network (ANN) for concrete containing RCA," Buildings **11**(8), 324 (2021).
[32]D. Zhang, D. Shi, F. Wang, D. Qian, Y. Zhou, J. Fu, M. Chen, D. Qiu, and S. Jiang, "Electromagnetic shocking induced fatigue improvement via tailoring the α-grain boundary in metastable β titanium alloy bolts," J. Alloys Compd. **966**, 171536 (2023).
[33]S. Afzali, M. Mohamadi-Baghmolaei, and S. Zendehboudi, "Application of gene expression programming (GEP) in modeling hydrocarbon recovery in WAG injection process," Energies **14**(21), 7131 (2021).
[34]X. Long, Z. Shen, J. Li, R. Dong, M. Liu, Y. Su, and C. Chen, "Size effect of nickel-based single crystal superalloy revealed by nanoindentation with low strain rates," J. Mater. Res. Technol. **29**, 2437–2447 (2024).
[35]Y. Peng, C. Yuan, X. Qin, J. Huang, and Y. Shi, "An improved gene expression programming approach for symbolic regression problems," Neurocomputing **137**, 293–301 (2014).
[36]G. Li, W. Chi, W. Wang, X. Liu, H. Tu, and X. Long, "High cycle fatigue behavior of additively manufactured Ti–6Al–4V alloy with HIP treatment at elevated temperatures," Int. J. Fatigue **184**, 108287 (2024).
[37]H. Malik and S. Mishra, "Application of gene expression programming (GEP) in power transformers fault diagnosis using DGA," IEEE Trans. Ind. Appl. **52**(6), 4556–4565 (2016).
[38]M. A. S. Hossain, M. N. Uddin, and M. M. Hossain, "Prediction of compressive strength fiber-reinforced geopolymer concrete (FRGC) using gene expression programming (GEP)," Mater. Today: Proc. (in press, 2023).
[39]Q. Guo, H. Hou, K. Wang, M. Li, P. K. Liaw, and Y. Zhao, "Coalescence of $Al_{0.3}CoCrFeNi$ polycrystalline high-entropy alloy in hot-pressed sintering: A molecular dynamics and phase-field study," npj Comput. Mater. **9**(1), 185 (2023).
[40]D. P. Singh, S. Mishra, and R. K. Porwal, "Parametric analysis through ANFIS modelling and optimization of micro-hole machining in super duplex stainless steel by die-sinking EDM," Adv. Mater. Process. Technol. **9**(4), 1885–1902 (2023).
[41]W. Yu, X. Chong, Y. Liang, X. Gao, Y. Wei, S. Shang, M. Gan, Y. Lin, A. Zhang, H. Wu, L. Chen, J. Feng, Z. K. Liu, and H. Song, "Discovering novel γ–γ′ Pt–Al superalloys via lattice stability in Pt_3Al induced by local atomic environment distortion," Acta Mater. **281**, 120413 (2024).
[42]S. Saha, S. R. Maity, and S. Dey, "Prediction of WEDM performances using clustering techniques in ANFIS during machining of A286 Superalloy," J. Inst. Eng. (India): Ser. C **104**(2), 315–326 (2023).
[43]N. Rajesh and R. Lokanadham, "Optimization of machining parameters and studies on characteristics of Monel k400 alloy using abrasive water jet Machining using ANFIS," Mater. Today: Proc. **98**, 40–46 (2024).
[44]D. Y. Pimenov, A. Bustillo, S. Wojciechowski, V. S. Sharma, M. K. Gupta, and M. Kuntoğlu, "Artificial intelligence systems for tool condition monitoring in machining: Analysis and critical review," J. Intell. Manuf. **34**(5), 2079–2121 (2023).
[45]L. Shao, X. Zhang, Y. Chen, L. Zhu, S. Wu, Q. Liu, W. Li, N. Xue, Z. Tu, T. Wang, J. Zhang, S. Dai, X. Shi, M. Chen, and T. Wang, "Why do cracks occur in the weld joint of Ti–22Al–25Nb alloy during post-weld heat treatment?," Front. Mater. **10**, 1135407 (2023).
[46]W. Yang, X. Jiang, X. Tian, H. Hou, and Y. Zhao, "Phase-field simulation of nano-α′ precipitates under irradiation and dislocations," J. Mater. Res. Technol. **22**, 1307–1321 (2023).
[47]D. Cica, B. Sredanovic, S. Tesic, and D. Kramar, "Predictive modeling of turning operations under different cooling/lubricating conditions for sustainable manufacturing with machine learning techniques," Appl. Comput. Inf. **20**(1/2), 162–180 (2024).
[48]W. Chen, H. Hou, Y. Zhang, W. Liu, and Y. Zhao, "Thermal and solute diffusion in α-Mg dendrite growth of Mg-5wt. %Zn alloy: A phase-field study," J. Mater. Res. Technol. **24**, 8401–8413 (2023).
[49]P. Agrawal and P. Jayaswal, "Diagnosis and classifications of bearing faults using artificial neural network and support vector machine," J. Inst. Eng. (India): Ser. C **101**(1), 61–72 (2020).
[50]V. C. Nguyen, T. D. Nguyen, and D. H. Tien, "Cutting parameter optimization in finishing milling of Ti–6Al–4V titanium alloy under MQL condition using TOPSIS and ANOVA analysis," Eng., Technol. Appl. Sci. Res. **11**(1), 6775–6780 (2021).